Harmonic Analysis of High-Tc Rf SQUID to Determine the Optimum Working Condition for Its Automatic Application

Jie Xu, Christian Benden, Yi Zhang, Jie Li and Hans-Joachim Krause

***Abstract*—High-Tc radio-frequency (rf) SQUIDs are well researched and have been utilized in a range of applications. The rf SQUID operating in nonhysteretic mode has been elaborated theoretically in a few of literatures, among which an effective method of harmonic analysis was presented to find its optimum working point. A suitable flux-to-voltage curve of the rf SQUID should be acquired before applying the harmonic analysis method, but the approach of getting the suitable curve is unclear. This paper carried out a analysis with respect to the three harmonics which primarily affect the waveform of flux-to-voltage curves and came to the condition which need be satisfied to acquire the desirable kind of curves. In which, the one with the largest value of its maximum transfer function could be considered as working in the optimum condition. Three rf SQUIDs were employed in experiment to demonstrate the detailed procedure of determining their optimum working conditions, which were the rf frequencies and the attenuator voltages of their tank circuits. Judging from the experimental results, the method proposed in this article is very effective, the optimum working conditions of the three rf SQUIDs can be accurately obtained. The findings would be instructional for automatically setting the working conditions of high-Tc rf SQUIDs in practical applications.**

***Index Terms*—Automatic settings of readout circuits, desirable flux-to-voltage curves, harmonic coefficients of characteristic expression, optimum working conditions for high-Tc rf SQUIDs.**

I. Introduction

RF SQUIDs (short for Radio-frequency Superconducting Quantum Interference Devices), which consist of a single Josephson junction closed with a superconducting loop, have been well studied [1] and achieved a range of applications in biomagnetism, nondestructive inspection, magnetic anomaly detection and so on. Rf SQUIDs have two different kinds of operating modes, namely hysteretic mode and nonhysteretic mode, which mainly depend on the value of SQUID parameter $\beta_{rf} = 2\pi L_{sq} I_c/\Phi_0$. For large values of the parameter β_{rf}, the SQUID is often in the hysteretic mode, also called dissipative mode, where the trapped flux in the SQUID is a multivalued function of the external flux. For small values of the parameter β_{rf}, the SQUID is often in the nonhysteretic mode (or called dispersive mode), characterized by a single-valued functional dependence of the trapped flux in the SQUID on the external flux. For instance, rf SQUIDs with intrinsically shunted grain-boundary junctions [2] exhibiting a small normal resistance and junction capacitance are usually nonhysteretic.

The rf SQUID operating in nonhysteretic mode has been elaborated theoretically in a few of literatures [1], [3]–[8]. However, in practice its optimum working point is usually determined by visual estimation after a set of manual adjustments, because some uncertain parameters (e.g. critical current I_c, coupling coefficient k) causing analytical solutions to be unavailable from the expression of its flux-to-voltage (U-ϕ) characteristics. Considering the inconvenient for practical applications, Xu et al. [9] started from the fundamental equations [3], [10] describing the rf SQUID and showed that its U-ϕ characteristic can be approximated with sufficient precision by just four coefficients. Thus, the optimum working point can be easily determined by analytical deduction from the harmonic expansion in theory and also by means of numerical fitting methods in experiment.

It is important to note that a suitable U-ϕ curve of the rf SQUID should be acquired before applying the above-mentioned harmonic analysis method. Whether the curve is suitable or not has relationship with three main factors: the maximum transfer function of dU/dϕ, peak-to-peak voltage and the regularity of its waveform. A desirable kind of U-ϕ curve is chosen by combining these factors to find a better overall performance. Besides, in practice one cannot change these factors directly but can adjust only a few settings on the SQUID readout electronics, for example, rf frequency and attenuator voltage. However, what kind of relationship between the theoretical factors and the operable settings? How can we find the optimum working condition for a certain rf SQUID? And what is the specific procedure? This paper will focus and answer these questions.

II. Theory

In our previous work, we presented a harmonic expansion to describe the flux-to-voltage characteristics of high-Tc rf SQUIDs in nonhysteretic mode by just four coefficients: the first three harmonic amplitudes and an offset, shown as [9]

$$U_D(\phi) = A_0 + A_1 cos(2\pi\phi) + A_2 cos(4\pi\phi) + A_3 cos(6\pi\phi) \quad (1)$$

In which, A_0 is an offset voltage; A_1, A_2 and A_3 are separately the coefficients of the fundamental, the second and the third harmonic components, given as

Manuscript received xxx xx, xxxx; revised xxx xx, xxxx; accepted xxx xx, xxxx. Date of current version xxx xx, xxxx.

J. Xu, C. Benden, Y. Zhang and H.-J. Krause are with Peter Grünberg Institute (PGI-8), Forschungszentrum Jülich, 52425 Jülich, Germany (*Corresponding Author: Hans-Joachim Krause*; E-mail: h.-j.krause@fz-juelich.de).

J. Xu and J. Li are with College of Mechatronic Engineering and Automation, National University of Defense Technology, 410073 Changsha, China.

Digital Object Identifier xx.xxxx/xxxx.xxxx.xxxxxxx

$$A_0 = \widetilde{\xi}\left(\frac{\widetilde{K}^2\widetilde{J}^2 cos^2\theta}{4I_D} + I_D\right) \quad (2)$$

$$A_1 = \widetilde{K}\widetilde{J}\widetilde{\xi}\left(\frac{3\widetilde{K}^2\widetilde{J}^2 sin\theta cos^2\theta}{8I_D^2} - sin\theta\right) \quad (3)$$

$$A_2 = \frac{\widetilde{K}^2\widetilde{J}^2\widetilde{\xi} cos^2\theta}{4I_D} \quad (4)$$

$$A_3 = \frac{\widetilde{K}^3\widetilde{J}^3\widetilde{\xi} sin\theta cos^2\theta}{8I_D^2} \quad (5)$$

with $\widetilde{K} = k^2Q\beta_{rf}/\pi$, $\widetilde{J} = J_1\left(2\pi I_D/\sqrt{\xi^2+1}\right)$, $\widetilde{\xi} = 1/\sqrt{\xi^2+1}$ and $\theta = tan^{-1}\xi$.

Here, the dimensionless quantities voltage U_D, current I_D, frequency ξ and flux ϕ are severally given by $U_D = MU_{rf}/(2\pi f L_t\Phi_0)$, $I_D = MQI_{rf}/\Phi_0$, $\xi = 2Q\Delta f/f_0$ and $\phi = \Phi_e/\Phi_0$. Besides, β_{rf} is the rf SQUID parameter expressed by $\beta_{rf} = 2\pi L_{sq}I_c/\Phi_0$; M is the mutual inductance between the tank circuit and the rf SQUID, which can be calculated by $M = k\sqrt{L_tL_{sq}}$; U_{rf} is the amplitude of the rf voltage across the tank circuit, I_{rf} is the amplitude of the applied rf current; L_t, f_0 and Q are severally the inductance, resonant frequency and quality factor of the tank circuit; f is the frequency of the rf current, Δf is the difference between f and f_0; L_{sq} is the inductance of the rf SQUID, k is coupling constant, and I_c is the critical current of the Josephson junction; Φ_e is the external magnetic flux threading the SQUID loop, Φ_0 is the magnetic flux quantum; J_1 denotes the Bessel function of the first kind.

In addition, we picked out six typical kinds of the measured flux-to-voltage curves in experiment and fitted them according to (1) with respect to their harmonics in the magnetic flux. The results were quite satisfactory, which validated that the harmonic expansion (1) was adequate to estimate the actual U-ϕ characteristics of high-Tc rf SQUIDs in nonhysteretic mode. Several typical kinds of U-ϕ curves (TC) which can be frequently observed in practice are shown in Fig. 1.

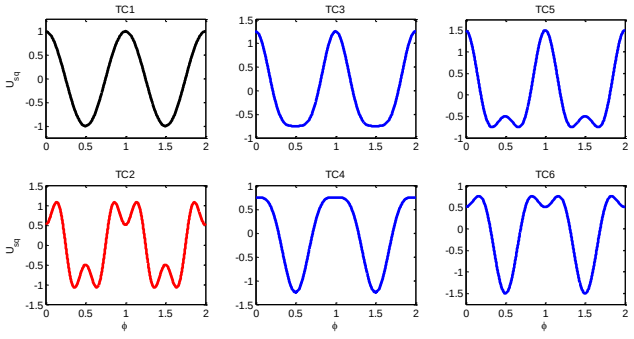

Fig. 1. Several typical kinds of U-ϕ curves frequently observed in practice.

In all the typical curves above, TC2 can be regarded as a desirable kind of U-ϕ curve on account of a better overall behavior in the maximum transfer function of dU/dϕ (TFm), peak-to-peak voltage (Upp) and the regularity of its waveform. In this case, the condition for acquiring this kind of U-ϕ curve ought to be explored in depth.

In regard to (1), since the waveform of U-ϕ curves only depends on A_1, A_2 and A_3, so the offset A_0 can be ignored naturally. Besides, in order to ensure the fundamental harmonic to be dominant in the waveform of U-ϕ curves, one can make a normalization of A_2/A_1 and A_3/A_1 and meet a condition of $|A_2/A_1| \leq 1$ and $|A_3/A_1| \leq 1$. As a result, (1) can be rewritten as

$$U(\phi) = cos(2\pi\phi) + \frac{A_2}{A_1}cos(4\pi\phi) + \frac{A_3}{A_1}cos(6\pi\phi) \quad (6)$$

A. Respective influence of the second and the third harmonic

It is easy to examine the respective influence of the both harmonics (A_2/A_1 and A_3/A_1) by enabling one of them to be zero and the other to change from -1 to 1, i.e., $A_3/A_1 = 0$, A_2/A_1 changes from -1 to 1 or $A_2/A_1 = 0$, A_3/A_1 changes from -1 to 1. Then, the corresponding TFm and Upp are shown in Fig. 2.

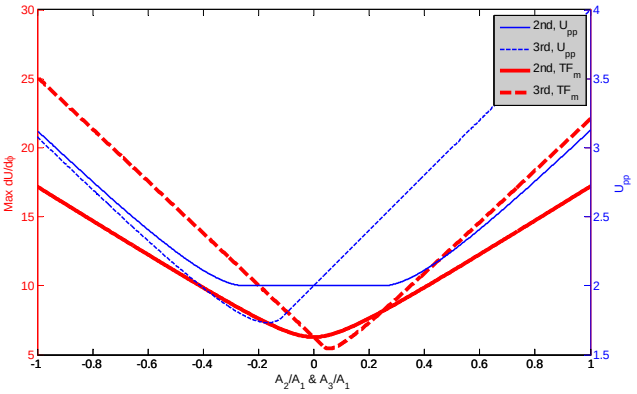

Fig. 2. Respective tendencies of TFm and Upp with respect to A_2/A_1 or A_3/A_1 (the left Y-axis Max dU/dϕ denotes TFm and used for the two red bold curves; the right Y-axis Upp is used for the two blue fine curves).

As can be seen from Fig. 2 if one analyzes and compares the four curves carefully:

- For the second harmonic: (a) when $|A_2/A_1|$ increases, TFm increases linearly with a slope of 10.9 from 6.3 to 17.2; (b) Upp remains unchanged firstly and then increases linearly with a slope of 1.5 from 2 to 3.1; (c) the relationships between TFm, Upp and A_2/A_1 are both even functions, which is obviously different from the third harmonic.
- For the third harmonic: (a) if $A_3/A_1 < 0$, when $|A_3/A_1|$ increases, TFm increases linearly with a slope of 20.8 from 6.3 to 25.1; while if $A_3/A_1 > 0$, TFm firstly decreases to the minimum value of 5.4 at 0.055ϕ and then increases linearly with a slope of 17.6 to 22.1; (b) the behavior of Upp is contrary to TFm and its rate of increment is almost the same as that of the second harmonic; (c) the increasing rate of TFm is nearly twice as much as that of the second harmonic.

- For either the second or the third harmonic, the increasing rate of TFm is much higher than that of Upp and its numerical values are also much larger than those of Upp.

In the cases of $A_3/A_1 = 0$, A_2/A_1 = -1, -0.5, 0, 0.5, 1 and $A_2/A_1 = 0$, A_3/A_1 = -1, -0.5, 0, 0.5, 1, the corresponding U-ϕ curves are shown in Fig. 3.

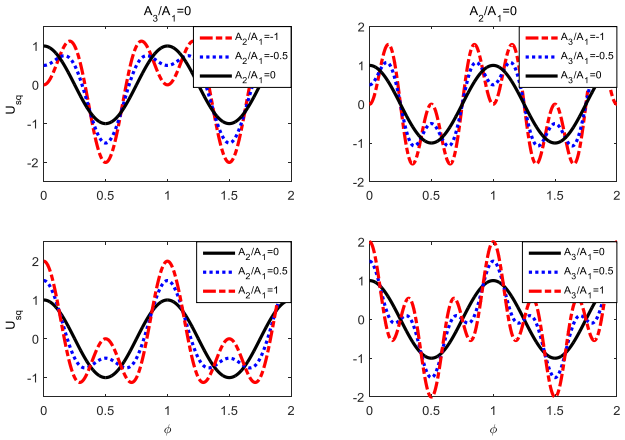

Fig. 3. U-ϕ curves based on the respective influence of A_2/A_1 or A_3/A_1.

As can be seen from Fig. 3:

- The desirable kind of U-ϕ curves (TC2) can be acquired under the condition of $A_2/A_1 = 0$ and $A_3/A_1 \subseteq$ [-1, 0).
- TC3 and TC5 can be acquired under the condition of $A_3/A_1 = 0$ and $A_2/A_1 \subseteq$ (0, 1]; TC4 and TC6 can be acquired under the condition of $A_3/A_1 = 0$ and $A_2/A_1 \subseteq$ [-1, 0).
- If $A_3/A_1 \subseteq$ (0, 1], the relevant U-ϕ curves would not be acceptable in any case of A_2/A_1.

B. Conjunct influence of the second and the third harmonics

If A_2/A_1 and A_3/A_1 are both changing from -1 to 1, the corresponding TFm and Upp are shown in Fig. 4.

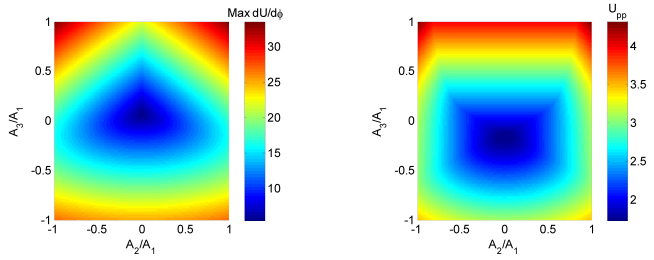

Fig. 4. Conjunct tendencies of TFm and Upp with respect to A_2/A_1 and A_3/A_1.

As can be seen from Fig. 4:

- For the both of TFm and Upp, their corresponding extreme points can be acquired under the condition of $|A_2/A_1| = 1$ and $|A_3/A_1| = 1$; The respective maximum values of 33.6 and 4.3 are achieved at the location of $A_3/A_1 = 1$ and $|A_2/A_1| = 1$.
- The features of TFm and Upp are both even functions with respect to A_2/A_1.

In the cases of A_2/A_1 = -0.5, 0.5, -1, 1, A_3/A_1 = -1, -0.5, 0, 0.5, 1 and A_3/A_1 = -0.5, 0.5, -1, 1, A_2/A_1 = -1, -0.5, 0, 0.5, 1, the corresponding U-ϕ curves are shown in Fig. 5.

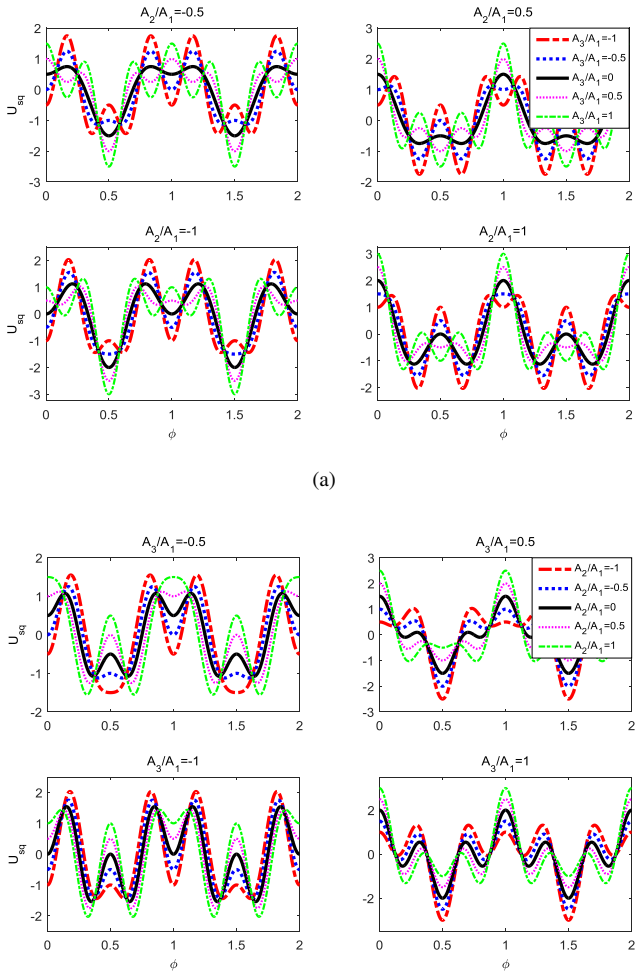

Fig. 5. U-ϕ curves based on the conjunct influence of A_2/A_1 and A_3/A_1: (a) A_2/A_1 = -0.5, 0.5, -1, 1, A_3/A_1 = -1, -0.5, 0, 0.5, 1; (b) A_3/A_1 = -0.5, 0.5, -1, 1, A_2/A_1 = -1, -0.5, 0, 0.5, 1.

As can be seen from Fig. 5:

- The desirable kind of U-ϕ curves can only be acquired under the condition of $A_3/A_1 \subseteq$ [-1, 0) and $|A_2/A_1| \leq |A_3/A_1|$.
- Although the second harmonic can enlarge TFm and Upp partly on the basis of the third harmonic, it also undermines the regularity and symmetry of original U-ϕ curves, which is unfavorable for determining the optimum working points.
- A sufficient condition for the optimum U-ϕ curve is A_3/A_1 = -1 and $A_2/A_1 = 0$.

C. Requirement for the basic parameters describing rf SQUIDs

Considering that a sufficient condition for acquiring the optimum U-ϕ curve has been presented as A_3/A_1 = -1 and $A_2/A_1 = 0$, in which, if A_1, A_2 and A_3 are severally replaced

by (3), (4) and (5), one can readily attain a set of equations as

$$\begin{cases} \left(\frac{k^2Q\beta_{rf}}{\pi}\right)^2 J_1^2\left(\frac{2\pi I_D}{\sqrt{\xi^2+1}}\right)\frac{cos^2(tan^{-1}\xi)}{I_D^2}=2 \\ \frac{I_D}{\sqrt{\xi^2+1}}=0 \end{cases} \tag{7}$$

Notice that if $I_D/\sqrt{\xi^2+1} = 0$, then $J_1\left(2\pi I_D/\sqrt{\xi^2+1}\right) = 0$, which is indicated as a contradiction and means the optimum U-ϕ curve can not be achieved in theory. Hence, (7) can be revised as

$$\begin{cases} \left(\frac{k^2Q\beta_{rf}}{\pi}\right)^2 J_1^2\left(\frac{2\pi I_D}{\sqrt{\xi^2+1}}\right)\frac{cos^2(tan^{-1}\xi)}{I_D^2}=2 \\ \frac{I_D}{\sqrt{\xi^2+1}}\to 0 \end{cases} \tag{8}$$

Similarly, in case of only acquiring the desirable kind of U-ϕ curves, which is under the condition of $A_3/A_1 \subseteq$ [-1, 0) and $|A_2/A_1| \le |A_3/A_1|$ (i.e. $|A_2| \le |A_3|$). Two cases should be considered individually as follows.

Case1: If $A_1 > 0$, then -$A_1 \le A_3 < 0$ and $|A_2| \le |A_3|$, namely one can achieve a set of inequalities as

$$\begin{cases} \widetilde{K}\widetilde{J}\widetilde{\xi}sin\theta < 0 \\ |\widetilde{K}\widetilde{J}cos\theta| \le \sqrt{2}|I_D| \\ |\widetilde{K}\widetilde{J}sin\theta| \ge 2|I_D| \end{cases} \tag{9}$$

Case2: If $A_1 < 0$, then $0 < A_3 \le$ -A_1 and $|A_2| \le |A_3|$, as a result, one will come at a conflict of $2\sqrt{6}/3|I_D| < |\widetilde{K}\widetilde{J}cos\theta| \le \sqrt{2}|I_D|$, which is obviously inconsistent and ought to be ignored here.

III. Experiment

At present, one can only search the optimum working condition (mainly rf frequency and attenuator voltage) by visual estimation after a set of manual adjustments for a typical readout electronics, which is inconvenient in practical applications. Now, it can be determined according to the criterion in Section II, exhibited as the following steps. The measurements were carried out using three rf SQUIDs introduced in [9] at 77 K, which had been chosen from some experimental rf SQUIDs, as shown in Fig. 6. The SQUIDs were operated with a typical readout electronics [11]. The total amplification of the SQUID electronics is about 105. A 200 Hz triangular signal with a peak-to-peak voltage of ± 1 V was employed to supply flux modulation via a coil.

Step1: Measuring the reflection condition of the tank circuit employed for an rf SQUID to obtain its resonant frequency f_0, as shown in Fig. 7.

As can be seen from Fig. 7, the resonant frequencies for the three rf SQUIDs are about 601.5, 624.5 and 551 MHz, respectively.

Step2: Adjusting rf frequency (Freq) in the vicinity of f_0 and attenuator voltage (ATT) simultaneously, and recording the actual U-ϕ curves in different combinations of Freq and ATT.

Fig. 6. Some experimental rf SQUIDs used for measurements

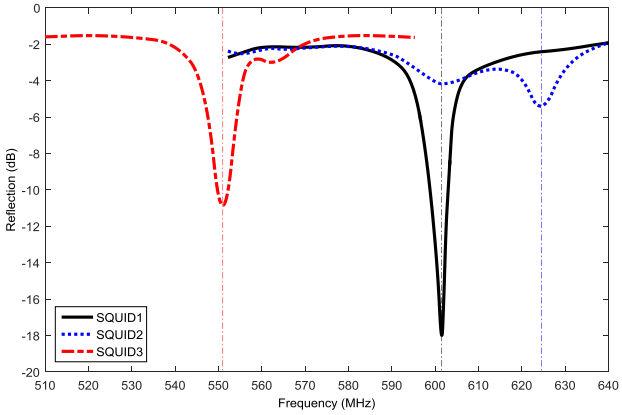

Fig. 7. Measured reflection of the tank circuits employed for the three rf SQUIDs.

Step3: Fitting the recorded U-ϕ curves on the basis of (1) to acquire the three harmonic coefficients: A_1, A_2 and A_3.

Step4: Picking out the desirable kind of U-ϕ curves depends on whether the condition of $A_3/A_1 \subseteq$ [-1, 0) and $|A_2| \le |A_3|$ has been satisfied or not.

Step5: In the desirable kind of U-ϕ curves selected from Step4, the one having the largest value of TFm can be considered as the U-ϕ curve in the optimum working condition.

The specific procedures and results of searching the optimum working condition (OWC) for the three rf SQUIDs were shown in Fig. 8.

Fig. 8 is actually a display of the above-mentioned Step2 to Step5. Here, SQUID1 in Fig. 8(a) will be taken as an example for detailed description. As can be seen from Fig. 8(a), the two sub-figures on the left show: under the different combinations of rf frequency (Freq) and attenuator voltage (ATT), the ratio distribution of three harmonic coefficients ($|A_2/A_1|$ and $|A_3/A_1|$) was obtained after the recorded U-ϕ curves were fitted on the basis of (1). Then, according to the judgment condition of $A_3/A_1 \subseteq$ [-1, 0) and $|A_2| \le |A_3|$, the combinations of Freq and ATT that meeting the condition were selected, as shown by the red stars in the sub-figure in the upper right corner. Each red star corresponds to a combination of Freq and ATT, and also corresponds to a recorded U-ϕ curve (i.e. desirable kind of U-ϕ curve). In these desirable kind of U-ϕ curves, the one having the largest value of TFm (dU/dϕ) was considered as the U-ϕ curve in the optimum

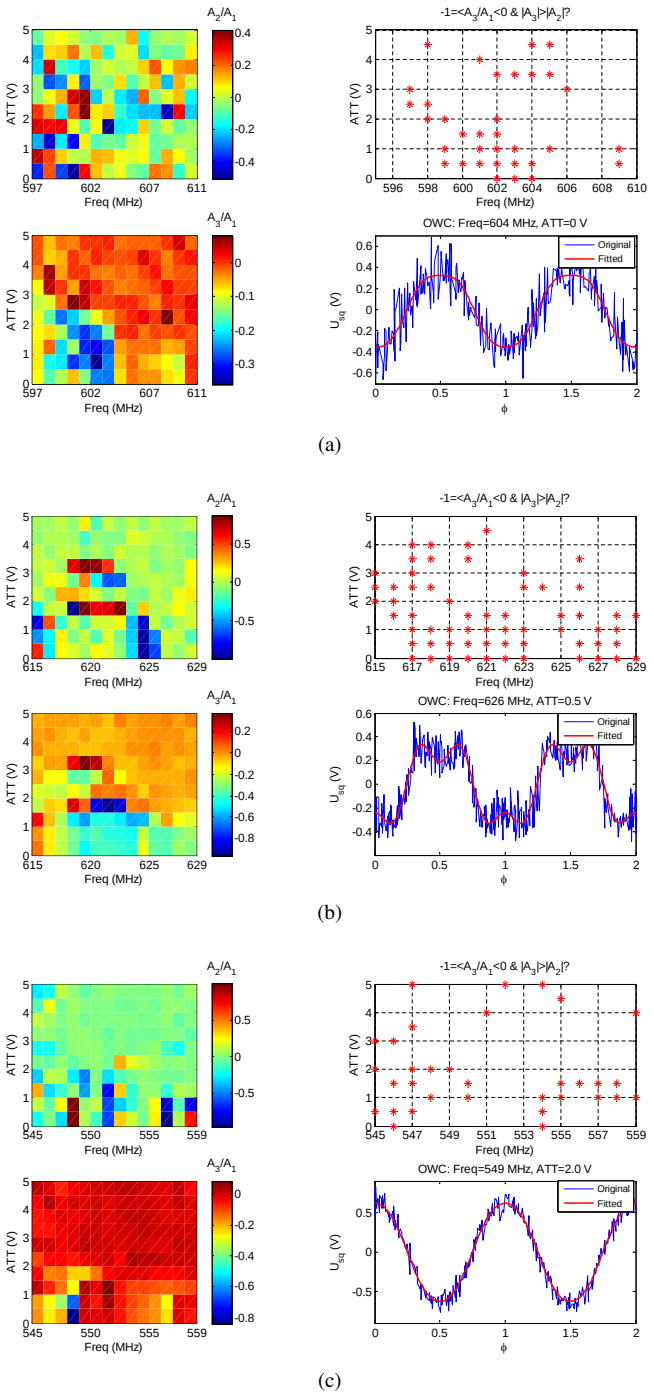

Fig. 8. Procedures and results of searching the optimum working condition for the three rf SQUIDs: (a) SQUID1; (b) SQUID2; (c) SQUID3.

working condition. For the SQUID1, its optimum working condition was readily determined according to this method: Freq=604 MHz & ATT=0 V, as shown in the sub-figure in the lower right corner (the blue line represents the original curve and the red line represents the curve after fitting). Similarly, the optimum working conditions for the other two SQUIDs were Freq=626 MHz & ATT=0.5 V (SQUID2) and Freq=549 MHz & ATT=2 V (SQUID3), as shown in Fig. 8(b) and Fig. 8(c) respectively.

IV. Discussion

As for a certain rf SQUID with a specific tank circuit, some of its basic parameters can be decided, e.g, β_{rf}, k and Q, so there will only be two variable parameters ξ and I_D in (3), (4) and (5). Here, $k^2Q\beta_{rf}/\pi$ might just as well equal 1.5 to make a distinction between its square (1.5^2) and cubic (1.5^3) items. The relationships between the three harmonic coefficients A_1, A_2 and A_3 with respect to ξ and I_D and the result of finding the desirable kind of U-ϕ curves are shown in Fig. 9.

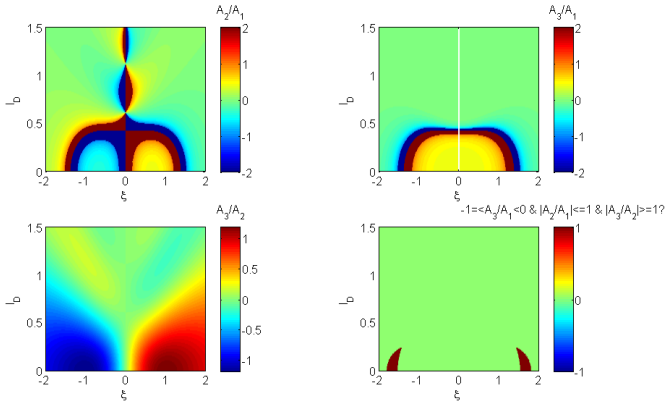

Fig. 9. Relationships between the three harmonic coefficients A_1, A_2 and A_3 with respect to ξ and I_D ($|A_2/A_1|$ and $|A_3/A_1|$ are less than 2) and the result of finding the desirable kind of U-ϕ curves.

As can be seen from Fig. 9, the optimum U-ϕ curve can only be acquired under the condition of $1.5 < |\xi| < 2$ and $0 < I_D < 0.25$. It is quite consistent with the measured results of the three rf SQUIDs in regard to Freq and ATT, in which, Δf and ATT are 2.5 MHz & 0 V, 1.5 MHz & 0.5 V and -2 MHz & 2 V, respectively.

If one changes the value of $k^2Q\beta_{rf}/\pi$, such as 0.5, 1, 1.4, 1.5, 2 and 3, their search results for the desirable kind of U-ϕ curves are shown in Fig. 10.

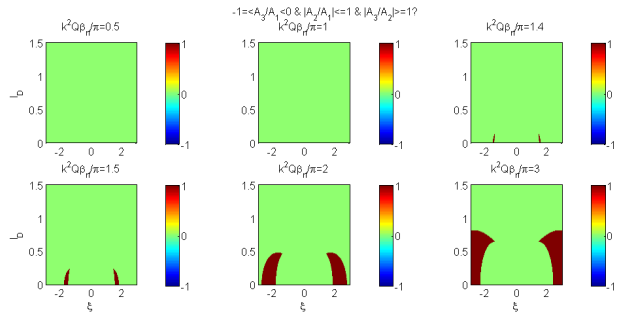

Fig. 10. Search results for the desirable kind of U-ϕ curves with different values of $k^2Q\beta_{rf}/\pi$.

As can be seen from Fig. 10, although small value of $k^2Q\beta_{rf}/\pi$ is a sufficient condition for the harmonic expansion, one might not acquire any desirable kind of U-ϕ curves in case that $k^2Q\beta_{rf}/\pi$ is too small.

In the content above, an essential premise is that the fundamental harmonic should be dominant in the waveform of U-ϕ curves, i.e., $|A_2/A_1| < 1$ and $|A_3/A_1| < 1$. However,

what if $|A_2/A_1| > 1$ or $|A_3/A_1| > 1$? Hence, in the cases of $A_3/A_1 = 0$, $A_2/A_1 = 1$, 2, 3, 5, 10 and $A_2/A_1 = 0$, $A_3/A_1 = 1$, 2, 3, 5, 10, the corresponding U-ϕ curves are shown in Fig. 11.

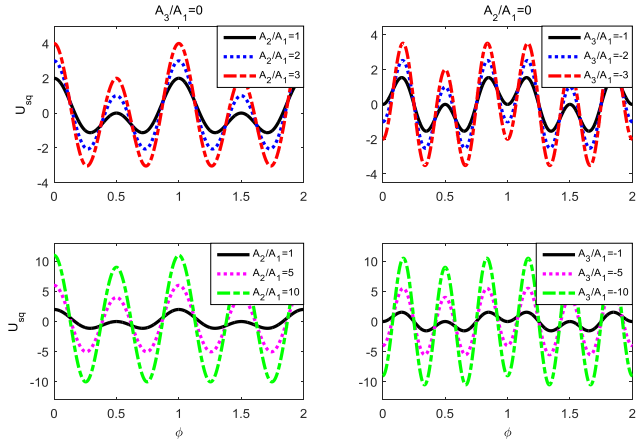

Fig. 11. U-ϕ curves on the basis of $|A_2/A_1| > 1$ or $|A_3/A_1| > 1$.

As can be seen from Fig. 11, if $|A_2/A_1| > 1$ or $|A_3/A_1| > 1$, there are commonly more than one comparative peaks or valleys in a period of ϕ, which is hardly observed in practice and inconvenient for determining the optimum working points.

In this article, the largest value of TFm was utilized as a criterion for selecting the optimum one from the desirable kind of U-ϕ curves. Certainly, one can also use other expressions for considering the both of TFm and Upp, for instance, $y = (1 - e^{-TFm/A})(1 - e^{-Upp/B})$ with two constants A and B.

In addition, Freq and ATT were divided with a step of 1 MHz and 0.5 V, respectively. One can surely divide them into slighter segments for the purpose of a higher precision in finding the optimum working condition. Also, the range of Freq can be expanded in a certain degree while ignoring the incremental calculation.

V. Conclusion

In consideration of the inconvenient to determine the optimum working condition (namely two pivotal settings on the SQUID readout electronics: rf frequency and attenuator voltage) of high-Tc rf SQUIDs in practice, an in-depth analysis with respect to the three harmonics (1st, 2nd and 3rd harmonic) which primarily affect the waveform of U-ϕ curves based on the previously proposed harmonic expansion of its flux-to-voltage characteristic was carried out. Desirable kind of U-ϕ curves would be acquired if the condition of $A_3/A_1 \subseteq$ [-1, 0) and $|A_2| \leq |A_3|$ (A_1, A_2 and A_3 are the coefficients of the three harmonics respectively) had been satisfied. In which, the one with the largest value of its maximum transfer function could be considered as the U-ϕ curve in the optimum working condition. According to the analytical conclusions, three rf SQUIDs were employed in experiment to demonstrate the detailed procedure of determining their optimum working conditions and good result was obtained as expectation. The findings presented in this paper would be of referential value for automatically setting the working conditions of high-Tc RF SQUIDs in their practical applications.

Acknowledgment

Xu Jie gratefully acknowledges financial support from China Scholarship Council.

References

[1] J. Clarke and A. I. Braginski, *The SQUID Handbook, Vol. I*. Weinheim: Wiley-VCH, 2004.

[2] Y. Zhang, W. Zander, J. Schubert *et al.*, "Operation of high-sensitivity radio frequency superconducting quantum interference device magnetometers with superconducting coplanar resonators at 77 k," *Applied Physics Letters*, vol. 71, no. 5, pp. 704–706, 1997.

[3] A. Barone and G. Paterno, *Physics and applications of the Josephson effect*. New York: John Wiley & Sons Inc., 1982.

[4] K. K. Likharev, *Dynamics of Josephson junctions and circuits*. Amsterdam: Gordon and Breach Science, 1986.

[5] P. K. Hansma, "Superconducting single-junction interferometers with small critical currents," *Journal of Applied Physics*, vol. 44, no. 9, pp. 4191–4194, 1973.

[6] ——, "Observability of Josephson pair-quasiparticle interference in superconducting interferometers," *Physical Review B*, vol. 12, no. 5, pp. 1707–1711, 1975.

[7] B. Chesca, "Theory of RF SQUIDS operating in the presence of large thermal fluctuations," *Journal of Low Temperature Physics*, vol. 110, no. 5-6, pp. 963–1001, 1998.

[8] R. Kleiner, D. Koelle, and J. Clarke, "A numerical treatment of the rf SQUID: I. General properties and noise energy," *Journal of Low Temperature Physics*, vol. 149, no. 5-6, pp. 230–260, 2007.

[9] J. Xu, C. Benden, Y. Zhang *et al.*, "Harmonic Analysis for Finding the Optimum Working Point of High-Tc RF SQUID," *IEEE Transactions on Applied Superconductivity*, vol. 26, no. 3, pp. 1–4, 2016.

[10] Y. Zhang, "RF-SQUIDs aus oxydkeramischen supraleitern: präparation und Charakterisierung (RF-SQUIDs from oxide-ceramic superconductors: preparation and characterization)," Ph.D. dissertation, Gießen University, 1990.

[11] H.-J. Krause, N. Wolters, and Y. Zhang, "Novel stable and reliable readout electronics for HTS rf SQUID," *Physics Procedia*, vol. 36, pp. 306–311, 2012.